Accepted Manuscript

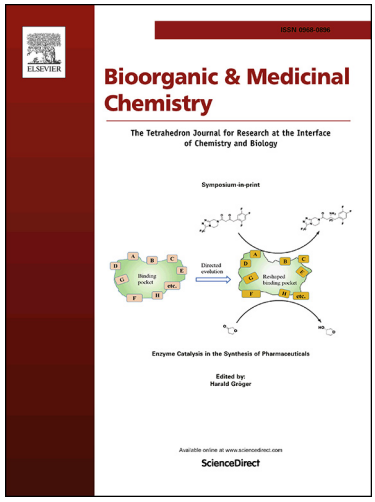

Conversion of Iodine to Fluorine-18 Based on Iodinated Chalcone and Evaluation for β-Amyloid PET Imaging

Sho Kaide, Masahiro Ono, Hiroyuki Watanabe, Yoichi Shimizu, Yuji Nakamoto, Kaori Togashi, Aiko Yamaguchi, Hirofumi Hanaoka, Hideo Saji

PII: S0968-0896(18)30507-8
DOI: https://doi.org/10.1016/j.bmc.2018.05.001
Reference: BMC 14343

To appear in: *Bioorganic & Medicinal Chemistry*

Received Date: 12 March 2018
Revised Date: 1 May 2018
Accepted Date: 2 May 2018

Please cite this article as: Kaide, S., Ono, M., Watanabe, H., Shimizu, Y., Nakamoto, Y., Togashi, K., Yamaguchi, A., Hanaoka, H., Saji, H., Conversion of Iodine to Fluorine-18 Based on Iodinated Chalcone and Evaluation for β-Amyloid PET Imaging, *Bioorganic & Medicinal Chemistry* (2018), doi: https://doi.org/10.1016/j.bmc.2018.05.001

Conversion of Iodine to Fluorine-18 Based on Iodinated Chalcone and Evaluation for β-Amyloid PET Imaging

Sho Kaide,[a] Masahiro Ono,[a,*] Hiroyuki Watanabe,[a] Yoichi Shimizu,[a,b] Yuji Nakamoto,[b,c] Kaori Togashi,[b,c] Aiko Yamaguchi,[d] Hirofumi Hanaoka,[d] & Hideo Saji[a]

[a] *Department of Patho-Functional Bioanalysis, Graduate School of Pharmaceutical Sciences, Kyoto University, 46-29 Yoshida Shimoadachi-cho, Sakyo-ku, Kyoto 606-8501, Japan*

[b] *Department of Radiology, Kyoto University Hospital, 54 Shogoin Kawahara-cho, Sakyo-ku, Kyoto 606-8507, Japan*

[c] *Department of Diagnostic Imaging and Nuclear Medicine, Graduate School of Medicine, Kyoto University, 54 Shogoin Kawahara-cho, Sakyo-ku, Kyoto 606-8507, Japan*

[d] *Department of Bioimaging Information Analysis, Gunma University Graduate School of Medicine, 3-39-22 Showa, Maebashi 371-8511, Japan*

[*]Corresponding author. Tel.: +81-75-753-4608. Fax: +81-75-753-4568. Email:

ono@pharm.kyoto-u.ac.jp

Abbreviations

Aβ, β-amyloid; AD, Alzheimer's disease; PET, positron emission tomography; SPECT, single photon emission computed tomography; DMFC, 4-dimethylamino-4'-fluoro-chalcone; FMC, 4'-fluoro-4-methylamino-chalcone; DMIC, 4-dimethylamino-4'-iodo-chalcone; IMC, 4'-iodo-4-methylamino-chalcone; FDA, Food and Drug Administration; HPLC, high-performance liquid chromatography; % ID/g, percentage injected dose per gram; BBB, blood-brain barrier; ARG, autoradiography; Tg, transgenic; KOH, potassium hydroxide; KOAc, potassium acetate; K_2CO_3, potassium carbonate; $(PdCl_2(dppf)CH_2Cl_2$, [1,1'-bis(diphenylphosphino)ferrocene]dichloropalladium(II), complex with dichloromethane; DMSO, dimethyl sulfoxide; DMF, *N*,*N*-dimethylformamide.

Abstract

In the amyloid cascade hypothesis, Aβ plaques are one of the major pathological biomarkers in the Alzheimer's disease (AD) brain. We report the synthesis and evaluation of novel radiofluorinated chalcones,

[^{18}F]4-dimethylamino-4'-fluoro-chalcone ([^{18}F]DMFC) and [^{18}F]4'-fluoro-4-methylamino-chalcone ([^{18}F]FMC), as β-amyloid (Aβ) imaging probes. The conversion of iodine directly introduced to the chalcone backbone into fluorine was successfully carried out by ^{18}F-labeling via the corresponding boronate precursors, achieving the direct introduction of fluorine-18 into the chalcone backbone to prepare [^{18}F]DMFC and [^{18}F]FMC. In a biodistribution study using normal mice, [^{18}F]DMFC and [^{18}F]FMC showed a higher initial uptake (4.43 and 5.47% ID/g at 2 min postinjection, respectively) into and more rapid clearance (0.52 and 0.66% ID/g at 30 min postinjection, respectively) from the brain than a Food and Drug Administration (FDA)-approved Aβ imaging agent ([^{18}F]Florbetapir), meaning the improvement of the probability of detecting Aβ plaques and the reduction of non-specific binding in the brain. In the *in vitro* binding studies using aggregates of recombinant Aβ peptides, [^{18}F]DMFC and [^{18}F]FMC showed high binding affinity to recombinant Aβ aggregates at the K_d values of 4.47 and 6.50 nM, respectively. In the *in vitro* autoradiography (ARG) experiment with AD brain sections, [^{18}F]DMFC and [^{18}F]FMC markedly accumulated only in a region with abundant Aβ plaques, indicating that they clearly recognized human Aβ plaques *in vitro*. These encouraging results suggest that [^{18}F]DMFC and [^{18}F]FMC may be promising PET probes for the

detection of an amyloid pathology and the early diagnosis of AD with marked accuracy.

Keywords

Alzheimer's disease; β-amyloid plaques; positron emission tomography; chalcones; ^{18}F-labeling

1. Introduction

Dementia affects 47 million people worldwide and this number is expected to increase to more than 131 million by 2050 as populations age, according to the World Alzheimer Report 2016.[1] Alzheimer's disease (AD) is the most common cause of dementia worldwide,[2] and the most typical neuropathological hallmarks in the AD brain are senile plaques composed of extracellular β-amyloid peptides (Aβ).[3] According to the amyloid cascade hypothesis, the accumulation of Aβ is an initiator in a multi-step pathological process, meaning that Aβ plaques are principal biomarkers and attractive targets for an early diagnosis of AD, assessment of therapeutic efficacy, and further understanding of the amyloid pathology.[4] In the past, a variety of imaging probes targeting Aβ plaques were developed for noninvasive imaging, including

positron emission tomography (PET) and single photon emission computed tomography (SPECT).[5] Among them, only three Aβ imaging agents for PET ([^{18}F]Flutemetamol,[6] [^{18}F]Florbetaben,[7] and [^{18}F]Florbetapir[8]) have been approved by the FDA, and tested clinically throughout the world. However, some clinical studies reported the clinical issue that they showed non-specific binding to white matter,[9, 10] resulting in the overestimation of PET signals and low accuracy of clinical diagnosis.

We previously developed various kinds of Aβ imaging probes based on chalcones and studied their structure-activity relationships.[11-17] Among them, the radioiodinated chalcones with an alkylamino group at 4-position, [^{125}I]4-dimethylamino-4'-iodo-chalcone ([^{125}I]DMIC, also abbreviated as [^{125}I]IDP-1 in our previous report[26]) and [^{125}I]4'-iodo-4-methylamino-chalcone ([^{125}I]IMC) (Figure 1A), displayed favorable characteristics as Aβ imaging probes. They can be easily formed by a one-pot condensation reaction and exhibit high *in vitro* affinity for Aβ plaques and moderate initial *in vivo* uptake into and rapid washout from the brain of normal mice.[17] In addition, iodine-125 has been directly introduced into chalcone backbones. Chalcones with the iodoallyloxy group at the 4'-position showed modest brain uptake into and slow washout from the brain,[12] suggesting that the direct introduction of iodine allowed favorable *in vivo* pharmacokinetics in the brain.

To the present, numerous methodologies to introduce fluorine-18 into organic compounds have been devised,[18] aiming at the development of structurally diverse and clinically relevant radiochemical compounds. In these contexts, some radiochemical strategies for the direct introduction of fluorine-18, including the preparation of radiofluorinated aromatic compounds via aryl iodonium ylides,[19] aryl sulfonium salts,[20] and aryl boronic precursors,[21] emerged and attracted much attention in molecular imaging studies. In addition to these advances of radiofluorination chemistry, copper-mediated ^{18}F-labeling of boronates derived from pinacol has recently been reported,[22] which enables the direct incorporation of fluorine-18 into an aromatic ring and may lead to preferable *in vivo* pharmacokinetics in the brain, as mentioned above. Boronates derived from pinacol are ideal precursors for ^{18}F-labeling as they are readily accessible from corresponding iodinated compounds and the commercially available copper complex $[Cu(OTf)_2(py)_4]$ (OTf = trifluoromethanesulfonate, py = pyridine) were used in this labeling reaction.[23] Therefore, the iodinated compounds can be used as starting materials in this method for the direct incorporation of fluorine-18 into an aromatic ring.

In this study, we applied this methodology to our original iodinated chalcones (DMIC and IMC), and synthesized novel radiofluorinated chalcones, [^{18}F]DMFC and

[^{18}F]FMC (Figure 1B), for the development of more useful Aβ imaging probes for PET with less non-specific binding in the AD brain. Then, we evaluated their utility as Aβ imaging probes by focusing on *in vitro* binding affinity in human brain tissues with AD pathology and *in vivo* pharmacokinetics in normal mice.

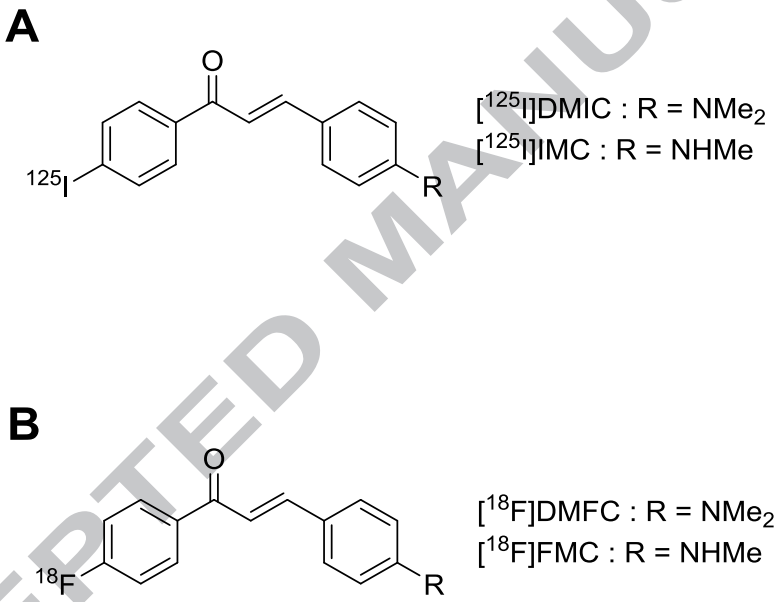

Figure 1. The chemical structural formula of radioiodinated chalcones, [^{125}I]DMIC and [^{125}I]IMC (A) and radiofluorinated chalcones, [^{18}F]DMFC and [^{18}F]FMC (B).

2. Results and Discussion

2.1. Chemistry

The synthesis of nonradioactive chalcones was carried out according to Scheme 1. 4-Iodoacetophenon was reacted with 4-dimethylaminobenzaldehyde or

4-methylaminobenzaldehyde in the presence of the basic catalyst (10% KOH) in ethanol at room temperature to form DMIC (**1**) or IMC (**2**) at yields of 63.4 and 60.2%, respectively. Boronate derivatives **3** and **4** as the precursors of ^{18}F-labeling were prepared from **1** and **2** by coupling reactions with bis(pinacolato)diboron in the presence of the base (KOAc) and palladium catalyst ($PdCl_2(dppf)CH_2Cl_2$) at yields of 35.0 and 41.6%, respectively, according to a method reported previously.[24] The fluorinated derivatives, 4-dimethylamino-4'-fluoro-chalcone (DMFC, **5**) and 4'-fluoro-4-methylamino-chalcone (FMC, **6**), were obtained from 4-fluoroacetophenon at yields of 65.0 and 76.7%, respectively.

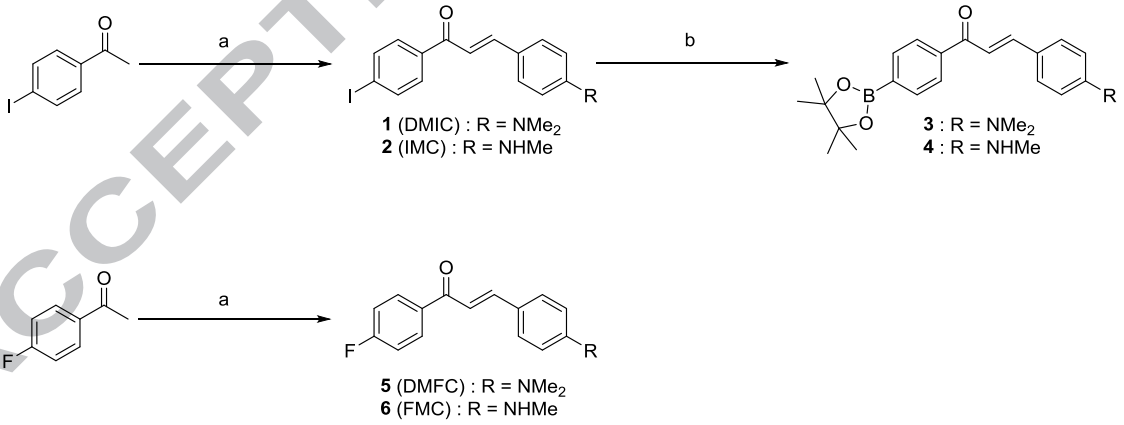

Scheme 1. Reagents: (a) 4-dimethylaminobenzaldehyde or 4-methylaminobenzaldehyde, 10% KOH, EtOH; (b) bis(pinacolato)diboron, KOAc, $PdCl_2(dppf)CH_2Cl_2$, DMSO.

The boronate derivatives (**3** and **4**) were used as the precursors of the copper-mediated nucleophilic ^{18}F-labeling in the successful preparation of [^{18}F]**5** ([^{18}F]DMFC) and [^{18}F]**6** ([^{18}F]FMC) according to Scheme 2, which facilitated the conversion from iodine directly introduced into the chalcone backbone into fluorine.

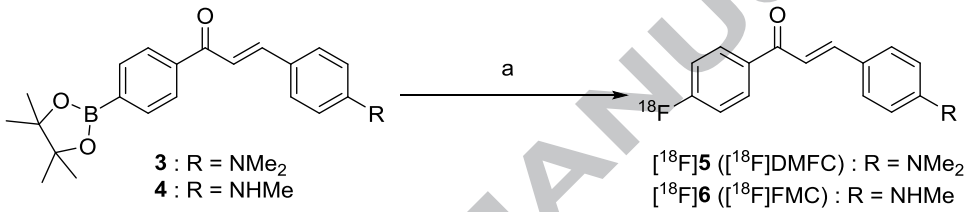

Scheme 2. Reagents: (a) $^{18}F^-$, K_2CO_3, Kryptofix 222, $Cu(OTf)_2(py)_4$, DMF.

The radiochemical identities of the desired radiofluorinated ligands were verified by reversed-phase high-performance liquid chromatography (HPLC) analysis. The radiochemical yields of [^{18}F]DMFC and [^{18}F]FMC were 37.0 and 45.0%, respectively, with radiochemical purities of >95% after purification by HPLC with specific activities of 1,256 and 466 GBq/μmol, respectively.

2.2. *In vivo* biodistribution study using normal mice

To evaluate the utility of [^{18}F]DMFC and [^{18}F]FMC as Aβ imaging probes for PET, we performed a biodistribution study in normal mice (Figure 2 and Table 1). For the

purpose of the detection of the amyloid pathology in the AD brain, promising Aβ imaging probes should show high initial uptake into and subsequent rapid washout from the brain because normal mice have no Aβ plaques in the brain.[25] The radioactivity accumulation of compounds is presented as the percentage injected dose per gram (% ID/g). [^{18}F]DMFC and [^{18}F]FMC displayed a higher initial brain uptake ($brain_{2\ min}$ = 4.43% ID/g and 5.47% ID/g, respectively) than the corresponding radioiodinated chalcones, [^{125}I]DMIC[26] (abbreviated as [^{125}I]IDP-1 in our previous report) and [^{125}I]IMC ($brain_{2\ min}$ = 2.43 and 3.52% ID/g, respectively) (Figure 2A, 2B, and Table 1). In general, some factors including the chemical structure, molecular charge, lipophilicity, and size have a marked influence on the compound's pharmacokinetics in the brain, indicating that the favorable permeability of the blood-brain barrier (BBB) of [^{18}F]DMFC (log P-value = 2.64 ± 0.01) and [^{18}F]FMC (log P-value = 2.25 ± 0.01) in comparison with [^{125}I]DMIC (log P-value = 3.16 ± 0.01) and [^{125}I]IMC (log P-value = 2.53 ± 0.01) may be due to the suitable lipophilicity and molecular size by conversion from iodine-125 to fluorine-18 at the 4'-position of the chalcone backbone.[27, 28] These novel radiofluorinated chalcones may meet the pharmacokinetic standards in the brain for clinical evaluations.[29, 30]

Then, clearance from the brain was evaluated by calculating the ratio of the

radioactivity accumulation at 2 and 30 min postinjection. [^{18}F]DMFC and [^{18}F]FMC exhibited higher brain$_{2\ min}$/brain$_{30\ min}$ ratios (8.5 and 8.3, respectively) than [^{125}I]DMIC[26] and [^{125}I]IMC (7.4 and 5.6, respectively) (Table 1), indicating that these radiofluorinated chalcones showed a more rapid clearance from the brain than radioiodinated forms. This may also be due to the suitable lipophilicity of the compound,[27, 28] resulting in less non-specific binding to white matter.

Then, [^{18}F]DMFC and [^{18}F]FMC were compared with fluoro-pegylated chalcone with dimethylamino group (FPEG chalcone) previously reported as an Aβ imaging probe.[14] In the previous study, ^{18}F-labeled FPEG chalcone displayed high initial brain uptake (brain$_{2\ min}$ = 3.48% ID/g) and subsequent clearance (brain$_{30\ min}$ = 1.08% ID/g).[14] However, the ratio of the radioactivity accumulation at 2 and 30 min postinjection was 3.2, which is much lower than that of [^{18}F]DMFC and [^{18}F]FMC. These results indicate that [^{18}F]DMFC and [^{18}F]FMC are less likely to show non-specific binding to white matter than ^{18}F-labeled FPEG chalcone. Furthermore, in comparison with a FDA-approved Aβ imaging agent, [^{18}F]Florbetapir (4.90% ID/g at 2 min postinjection and 3.0 for brain$_{2\ min}$/brain$_{30\ min}$ ratio),[31] [^{18}F]DMFC and [^{18}F]FMC were superior to [^{18}F]Florbetapir from the perspective of *in vivo* uptake into and washout from the brain (Figure 2C and Table 1), suggesting that these radiofluorinated chalcones in this study

may be clinically useful Aβ imaging probes.

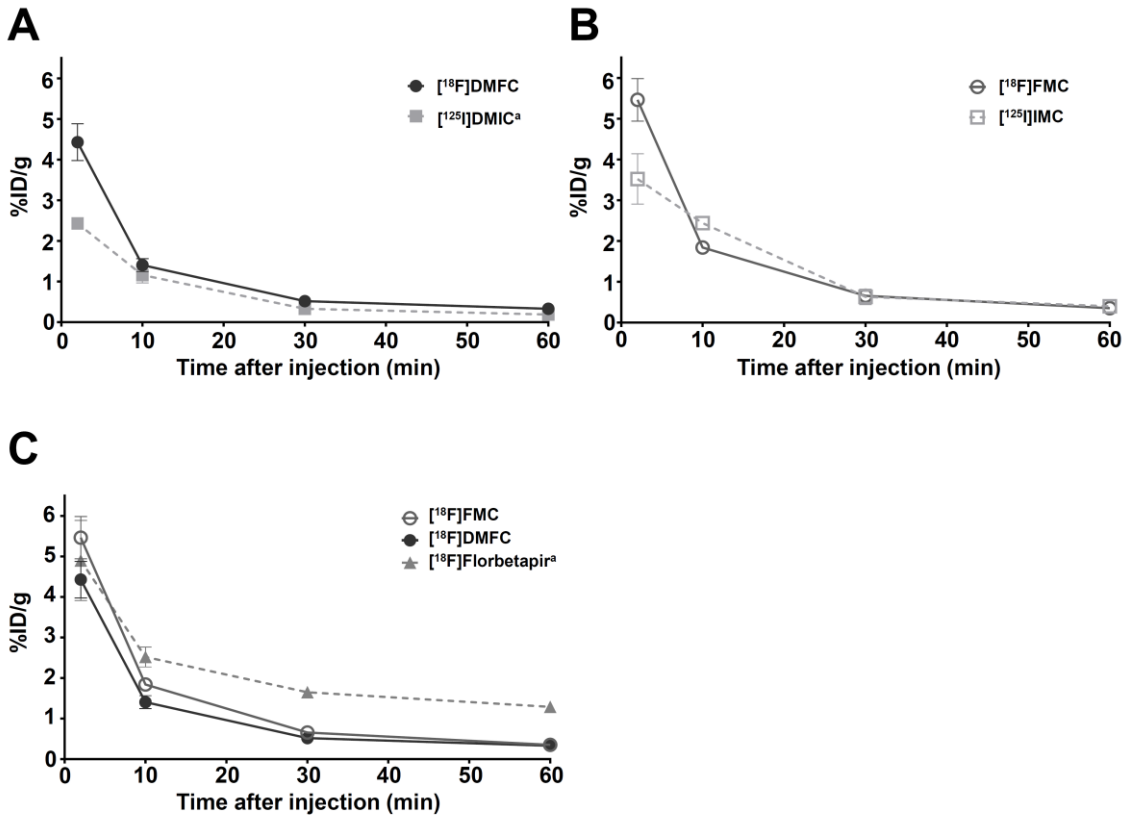

Figure 2. Comparison of brain uptake and clearance of [^{18}F]DMFC with [^{125}I]DMIC (A), [^{18}F]FMC with [^{125}I]IMC (B), and [^{18}F]DMFC [^{18}F]FMC with [^{18}F]Florbetapir (C) in normal mice (n = 5).

[a]The data of [^{125}I]DMIC and [^{18}F]Florbetapir were previously reported.[26, 31]

Table 1. Brain uptake of radioactivity after the injection of [^{18}F]chalcones, [^{125}I]chalcones and [^{18}F]Florbetapir in normal mice[a] and the 2 min/30 min ratio of

radioactivity accumulation.

Compd	%ID/g Brain		Ratio (2 min/30 min)
	2 min	30 min	
[^{18}F]DMFC	4.43 (0.45)	0.52 (0.07)	8.5
[^{125}I]DMIC	2.43 (0.10)	0.33 (0.07)	7.4
[^{18}F]FMC	5.47 (0.52)	0.66 (0.09)	8.3
[^{125}I]IMC	3.52 (0.62)	0.63 (0.19)	5.6
[^{18}F]Florbetapir	4.90 (0.99)	1.65 (0.11)	3.0

[a]Each value represents the mean (SD) of five animals.

The biodistribution of radioactivity in the whole body of [^{18}F]DMFC and [^{18}F]FMC was evaluated (Table S1). They accumulated initially in the liver ($liver_{2\ min}$ = 8.56 and 8.96% ID/g, respectively) and kidney ($kidney_{2\ min}$ = 8.52 and 9.21% ID/g, respectively) and subsequently in the intestine ($intestine_{60\ min}$ = 12.0 and 15.0% ID/g, respectively) as well as other lipophilic compounds. No marked accumulation in the bone was observed ($bone_{60\ min}$ = 1.65 and 1.86% ID/g, respectively). On the other hand, the radioactivity accumulation of ^{18}F-labeled FPEG chalcone in the bone increased over time and was higher ($bone_{60\ min}$ = 3.58% ID/g) than that of [^{18}F]DMFC and [^{18}F]FMC.

This difference could be attributable to the different physicochemical characteristics of their radiometabolites produced through some unclear physiological processes. These results indicate that [^{18}F]DMFC and [^{18}F]FMC are more stable toward defluorination *in vivo* than ^{18}F-labeled FPEG chalcone, and the introduction of fluorine-18 directly into chalcone backbone without PEG is suitable for the development of chalcone derivatives as Aβ imaging probes. On the basis of the biodistribution study in normal mice, [^{18}F]DMFC and [^{18}F]FMC displayed satisfactory pharmacokinetics *in vivo* as Aβ imaging probes for PET.

In order to confirm that these novel radiofluorinated chalcones permeated the blood-brain barrier (BBB) early followed by fast washout, a small-animal μPET imaging study of [^{18}F]DMFC was carried out in a normal mouse (Figure S1 and S2). The PET imaging data demonstrated that [^{18}F]DMFC rapidly passed through the BBB, penetrated at 2 min postinjection, and no radioactivity accumulation in any brain regions was observed at 30 min postinjection (Figure S1). The time activity curves (TACs) showed that [^{18}F]DMFC subsequently faded away from the brain to the level of a background by 30 min postinjection (Figure S2A). The PET images and TACs indicate that [^{18}F]DMFC showed little or no non-specific binding in the brain, leading to complete washout from the brain. TACs of other important tissues are shown in

Figure S2B. These results of the PET imaging study were consistent with those of the biodistribution study mentioned above, strongly suggesting that novel radiofluorinated chalcones may function well as useful Aβ imaging probes for PET *in vivo*.

2.3. Binding studies using Aβ aggregates in solution

Binding studies of [^{18}F]DMFC and [^{18}F]FMC to $A\beta_{1-42}$ aggregates were carried out in order to calculate their B_{max} and dissociation constant (K_d) values. The B_{max} and K_d values of [^{18}F]DMFC were 0.41 pmol/mg protein and 4.47 nM, respectively. The B_{max} and K_d values of [^{18}F]FMC were 0.42 pmol/mg protein and 6.50 nM, respectively. The K_d values of both compounds were as low as that of [^{3}H]PiB (K_d = 4.7 nM),[32] suggesting that their binding affinity to $A\beta_{1-42}$ aggregates is high enough to function as Aβ imaging probes. In the previous report, inhibition constant (K_i) values of DMFC and FMC for $A\beta_{1-42}$ aggregates in solution were 49.8 and 234.2 nM, respectively[14], indicating that they showed moderate binding affinity for recombinant $A\beta_{1-42}$ aggregates. These discrepancies are probably due to the difference of experimental conditions such as competitive ligands, buffer materials, and $A\beta_{1-42}$ aggregates. Moreover, the B_{max} values of [^{18}F]DMFC and [^{18}F]FMC were almost same, indicating that [^{18}F]DMFC and [^{18}F]FMC bound to the same binding sites in recombinant $A\beta_{1-42}$

aggregates.

2.4. *In vitro* autoradiography (ARG) with AD brain sections

For the clinical application of [^{18}F]DMFC and [^{18}F]FMC as Aβ imaging probes to precisely detect Aβ plaques in the human brain, we investigated their binding affinity to Aβ plaques by performing an *in vitro* ARG experiment with AD brain sections (Figure 3). In the *in vitro* autoradiograms, radioactivities of [^{18}F]DMFC and [^{18}F]FMC accumulated exactly along the gray matter of the frontal lobe (Figure 3A and 3B, respectively). Conversely, marked radioactivity accumulation was not observed in other regions such as the white matter, suggesting that [^{18}F]DMFC and [^{18}F]FMC selectively accumulated in the gray matter of the frontal lobe. [^{18}F]DMFC and [^{18}F]FMC showed no radioactive accumulation in the normal human brain sections (Figure S3). To confirm that this selectivity is derived from Aβ plaques, immunohistochemical staining with anti-Aβ antibody was carried out using adjacent sections, and the extensive accumulation of Aβ plaques was observed in the gray matter of the frontal lobe (Figure 3C), in accordance with the accumulation pattern of radioactivities of [^{18}F]DMFC and [^{18}F]FMC. These results indicate that [^{18}F]DMFC and [^{18}F]FMC sensitively recognized Aβ plaques in the AD brain *in vitro*.

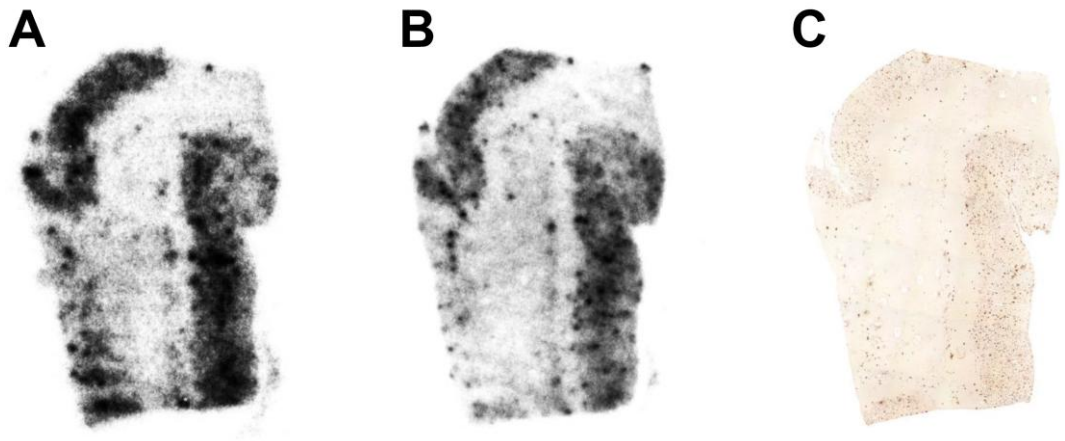

Figure 3. *In vitro* autoradiograms of AD brain sections labeled with [^{18}F]DMFC (A) and [^{18}F]FMC (B). Immunohistochemical staining using an anti-Aβ_{1-42} antibody (C).

We also carried out *in vitro* ARG with the Tg2576 brain section to investigate their binding ability against Aβ plaques in mice brain. [^{18}F]DMFC with higher binding affinity against Aβ aggregates than [^{18}F]FMC was used in this experiment. Compared to the marked labelling of Aβ plaques in human brain, [^{18}F]DMFC slightly showed binding affinity to Aβ plaques in the Tg2576 mouse brain (Figure S4). These discrepancies may be partially due to the difference in conformation of the aggregates formed by recombinant Aβ peptides, Aβ plaques in mice and human[33, 34]; however, details remain unclear. Irrespective of this, the encouraging data on AD brain sections support the potential clinical use in humans of these novel radiofluorinated chalcones.

3. Conclusion

In conclusion, novel radiofluorinated chalcones ([^{18}F]DMFC and [^{18}F]FMC) were designed as PET probes to detect Aβ plaques with low non-specific binding by the translation of iodine into fluorine. In order to achieve the objective, our original iodinated chalcones (DMIC and IMC) were used as starting materials, and the incorporation of fluorine-18 directly into the 4'-position of the chalcone backbone was successfully performed via novel copper-mediated radiofluorination chemistry. In the biodistribution study and PET imaging study with normal mice, they showed desirable [*in vivo* pharmacokinetics in the brain, partially due to the adjustment of the lipophilicity and molecular size by conversion from iodine into fluorine. In the binding studies using Aβ aggregates, their K_d values against Aβ aggregates were very low, indicating their high binding affinity to recombinant Aβ aggregates. In the *in vitro* ARG experiment using human brain sections with AD pathology, they intensely labeled Aβ plaques and did not markedly accumulate in regions without Aβ plaques. These encouraging *in vitro* and *in vivo* data suggest that [^{18}F]DMFC and [^{18}F]FMC may be useful for accurate PET imaging of Aβ plaques in the AD brain.

4. Experimental section

4.1. General information

All reagents were commercial products used without further purification. All compounds were purified by Smart Flash EPCLC W-Prep 2XY (Yamazen Corporation, Tokyo, Japan) unless indicated otherwise. ^{1}H and ^{13}C NMR spectra were recorded on a JNM-ECS400 (JEOL, Tokyo, Japan) with tetramethyl silane (TMS) as an internal standard. Coupling constants are reported in Hertz. Multiplicity was defined as singlet (s), doublet (d), triplet (t), or multiplet (m). ESI mass spectrometry was conducted with a SHIMADZU LCMS-2020. High-resolution mass spectrometry (HRMS) was carried out with a JEOL JMS-700 (JEOL, Tokyo, Japan). HPLC was performed with a Shimadzu system (an LC-20AD pump with an SPD-20A UV detector, λ = 254 nm) using a Cosmosil C_{18} column (Nacalai Tesque, COSMOSIL $5C_{18}$-MS-II 4.6 mm I.D. × 150 mm). All key compounds were proven by this method to show > 95% purity. Male ddY mice were purchased from Japan SLC, Inc. (Shizuoka, Japan), and were fed standard chow and had free access to water. We made all efforts to minimize suffering. Animal experiments were conducted in accordance with our institutional guidelines and were approved by Kyoto University. Experiments involving human subjects were performed in accordance with relevant guidelines and regulations and were approved

by the ethics committee of Kyoto University. Postmortem brain tissues from an autopsy-confirmed case of AD (73-year-old male) and a control subject (82-year-old female) were purchased from BioChain Institute Inc (California, USA).

4.1.1. (*E*)-3-(4-(Dimethylamino)phenyl)-1-(4-iodophenyl)-2-propen-1-one (1). 4-Iodoacetophenon (738 mg, 3.00 mmol) and 4-dimethylaminobenzaldehyde (447 mg, 3.00 mmol) were dissolved in 24 mL of ethanol. The mixture was stirred for 10 min in an ice bath. A 10-mL aliquot of 10% aqueous potassium hydroxide solution was then slowly added dropwisely to the reaction mixture. The reaction solution was stirred at room temperature for 9 h. A precipitate was collected and washed with 50% ethanol to give 717 mg of **1** (63.4%). ^{1}H NMR (400 MHz, $CDCl_3$) δ 7.85-7.77 (m, 3H), 7.72 (d, *J* = 8.4 Hz, 2H), 7.55 (d, *J* = 8.8 Hz, 2H), 7.25 (d, *J* = 5.6 Hz, 1H), 6.69 (d, *J* = 9.2 Hz, 2H), 3.05 (s, 6H). MS (ESI) m/z 378.3 [MH^+].

4.1.2. (*E*)-3-(4-(Methylamino)phenyl)-1-(4-iodophenyl)-2-propen-1-one (2). The same reaction as described above to prepare **1** was used, and 183 mg of **2** (60.2%) was obtained from 4-iodoacetophenon and 4-methylaminobenzaldehyde. ^{1}H NMR (400 MHz, $CDCl_3$) δ 7.84 (d, *J* = 8.0 Hz, 2H), 7.78 (d, *J* = 15.6 Hz, 1H), 7.72 (d, *J* = 8.4 Hz,

2H), 7.51 (d, *J* = 8.8 Hz, 2H), 7,25 (d, *J* = 8.8 Hz, 1H), 6.60 (d, *J* = 8.4 Hz, 2H), 4.18 (s, 1H), 2.90 (s, 3H). MS (ESI) m/z 364.3 [MH^+].

4.1.3.

(*E*)-3-(4-(Dimethylamino)phenyl)-1-(4-(4,4,5,5-tetramethyl-1,3,2-dioxaborolan-2-yl)phenyl)-2-propen-1-one (3). To a solution of **1** (487 mg, 1.29 mmol) in DMSO (anhydrous, 10 mL) were added bis(pinacolato)diboron (361 mg, 1.42 mmol), potassium acetate (380 mg, 3.87 mmol) and [1,1'-bis(diphenylphosphino)ferrocene]dichloropalladium(II), complex with dichloromethane ($PdCl_2(dppf)CH_2Cl_2$, 148 mg, 0.18 mmol). The mixture was stirred under reflux for 4 h. After being cooled to room temperature, the mixture was extracted with ethyl acetate (2×50 mL). The organic layers were combined and dried over Na_2SO_4. Evaporation of the solvent afforded a residue, which was purified by silica gel chlomatography (hexane/ethyl acetate = 4:1) to give 60.0 mg of **3** (35.0%). ^{1}H NMR (400 MHz, $CDCl_3$) δ 7.98 (d, *J* = 2.8 Hz, 2H), 7.91 (d, *J* = 8.4 Hz, 2H), 7.75 (d, *J* = 8.8 Hz, 1H), 7.55 (d, *J* = 9.2 Hz, 2H), 7.33 (d, *J* = 15.6 Hz, 1H), 3.05 (s, 6H), 1.37 (s, 12H). MS (ESI) m/z 378.3 [MH^+].

4.1.4.

(*E*)-3-(4-(Methylamino)phenyl)-1-(4-(4,4,5,5-tetramethyl-1,3,2-dioxaborolan-2-yl) phenyl)-2-propen-1-one (4). The same reaction as described above to prepare **3** was used, and 45.3 mg of **4** was obtained (41.6%) from **2**. ^{1}H NMR (400 MHz, $CDCl_3$) δ 7.97 (d, *J* = 7.2 Hz, 2H), 7.92 (d, *J* = 7.2 Hz, 2H), 7.76 (d, *J* = 15.2 Hz, 1H), 7.50 (d, *J* = 8.0 Hz, 2H), 7.32 (d, *J* = 15.6 Hz, 1H), 6.58 (d, *J* = 7.6 Hz, 2H), 4.22 (s, 1H), 2.88 (s, 3H), 1.36 (s, 12H). MS (ESI) m/z 364.3 [MH^+].

4.1.5. (*E*)-3-(4-(Dimethylamino)phenyl)-1-(4-fluorophenyl)-2-propen-1-one (5, DMFC). 4-Fluoroacetophenon (414 mg, 3.00 mmol) and 4-dimethylaminobenzaldehyde (447 mg, 3.00 mmol) were dissolved in 24 mL of ethanol. The mixture was stirred for 10 min in an ice bath. A 15-mL aliquot of 10% aqueous potassium hydroxide solution was then slowly added dropwisely to the reaction mixture. The reaction solution was stirred at room temperature for 9 h. A precipitate was collected and washed with 50% ethanol to give 525 mg of **5** (65.0%). ^{1}H NMR (400 MHz, $CDCl_3$) δ 8.06-8.02 (m, 2H), 7.80 (d, *J* = 15.6 Hz, 1H), 7.55 (d, *J* = 8.8 Hz, 2H), 7.30 (d, *J* = 15.2 Hz, 1H), 7.16 (t, *J* = 8.8 Hz, 2H), 6.70 (d, *J* = 8.8 Hz, 2H), 3.05 (s, 6H). ^{13}C NMR (100 MHz, $CDCl_3$) δ 188.9, 166,5, 164.0, 152.1, 146.0,

135.3, 130.5, 122.4, 116.2, 115.4, 111.8, 40.1. MS (ESI) m/z 270.2 [MH^+]. HRMS (FAB) m/z calcd. for $C_{17}H_{17}FNO$ 270.1294, found 270.1291.

4.1.6. (*E*)-3-(4-(Methylamino)phenyl)-1-(4-fluorophenyl)-2-propen-1-one (6, FMC).

The same reaction to prepare **5** was used, and 39.1 mg of **6** (76.7%) was obtained from 4-fluoroacetophenon and 4-methylaminobenzaldehyde. ^{1}H NMR (400 MHz, $CDCl_3$) δ 8.06-8.02 (m, 2H), 7.78 (d, *J* = 15.6 Hz, 1H), 7.52 (d, *J* = 8.8 Hz, 2H), 7.30 (d, *J* = 15.6 Hz, 1H), 7.18-7.14 (m, 2H), 6.60 (d, *J* = 8.8 Hz, 2H), 4.17 (s, 1H), 2.90 (s, 3H). ^{13}C NMR (100 MHz, $CDCl_3$) δ 190.3, 154.1, 151.5, 132.3, 130.6, 126.4, 123.6, 116.4, 115.4, 112.1, 111.4, 30.0. MS (ESI) m/z 256.1 [MH^+]. HRMS (FAB) m/z calcd. for $C_{16}H_{15}FNO$ 256.1138, found 256.1134.

4.2. Radiofluorination

The [^{18}F]fluoride was produced by a cyclotron (CYPRIS HM-12, Sumitomo Heavy Industries, Tokyo) via an $^{18}O(p,n)^{18}F$ reaction and passed through a Sep-Pak Light QMA cartridge (Waters) as an aqueous solution in ^{18}O-enriched water. The cartridge was dried by nitrogen gas, and the ^{18}F activity was eluted with 300 μL of 66 mM K_2CO_3 solution. Kryptofix222 (8.0 mg) was dissolved in the solution of [^{18}F]fluoride

in water. The solvent was removed at 120 °C under a stream of nitrogen gas. The residue was azeotropically dried with 300 μL of anhydrous acetonitrile three times at 120°C under a stream of nitrogen gas. A solution of the boronate precursor **3** or **4** (5.0 mg) and $Cu(OTf)_2(py)_4$ (9.0 mg) in *N*,*N*-dimethylformamide (DMF) (200 μL) was added to the reaction vessel containing the [^{18}F]fluoride activity. The mixture was heated at 110°C for 20 min. After passing the filter, the radiofluorinated ligand was purified by HPLC on a COSMOSIL 5C_{18}-MS-II column with an isocratic solvent of acetonitrile/H_2O (60/40 or 45/55, respectively) at a flow rate of 1.0 mL/min.

4.3. *In vivo* biodistribution study in normal mice

A saline solution (100 μL) of [^{18}F]DMFC or [^{18}F]FMC (111 - 112 kBq) containing ethanol (10.0 μL) and Tween 80 (0.100 μL) was directly injected intravenously into the tails of ddY mice (5 weeks old, male). The mice were sacrificed at various time points postinjection. The organs of interest were removed and weighed, and the radioactivity was measured with an automatic γ counter (Wallac WIZARD 1470, PerkinElmer).

4.4. Binding studies using Aβ aggregates in solution

$A\beta_{1-42}$ was purchased from the Peptides Institute, Inc. (Osaka, Japan). $A\beta_{1-42}$ aggregates were prepared by incubating the $A\beta_{1-42}$ peptide (0.25 mg mL^{-1} in PBS, pH 7.4) at 37 °C for 42 h with gentle and constant shaking. The reaction mixture contained increasing concentrations of [^{18}F]DMFC or [^{18}F]FMC (1.56-50.0 nM, 100 µL, DMSO), a fixed concentration of $A\beta_{1-42}$ aggregates (9.2 nM, 50 µL, PBS), and 10% EtOH (850 µL). Nonspecific binding was defined in the presence of 4 µM nonradioactive DMFC or FMC. After incubating for 3 h at room temperature, the solution was filtered through GF/B filters using an M-24 cell harvester. The radioactivities of the bound [^{18}F]DMFC and [^{18}F]FMC were measured with a γ counter (Wizard 1470, PerkinElmer). The B_{max} and K_d values were determined by using GraphPad Prism 5.0 (GraphPad Software, San Diego, CA, USA).

4.5. Immunohistochemical staining using AD brain sections

We performed immunohistochemical staining of brain sections according to a method reported previously.[27] Post-mortem brain sections of paraffin-embedded blocks from an autopsy-confirmed case of AD (73-year-old male) were used for staining. The sections were subjected to two 15-min incubations in xylene, two 1-min incubations in 100% EtOH, one 1-min incubation in 90% EtOH, and one 1-min incubation in 70%

EtOH to completely deparaffinize them, followed by two 2.5-min washes in water. They were then autoclaved for 15 min in 0.01 M citric acid buffer (pH 6.0) and incubated with 90% formic acid for 5 min to activate the antigen. After 2-min incubations in PBS-Tween 20, the sections were incubated at room temperature with an anti-$A\beta_{1-42}$ (BC05, Wako) primary antibody for 1 h. After three 5-min incubations in PBS-Tween 20, they were incubated with goat anti-mouse IgG (Histofine Simple Stain Mouse MAX-PO (MULTI), Nichirei Biosciences Inc.) at room temperature for 30 min. After three 3-min incubations in PBS-Tween 20 and one 5-min incubation in TBS, the sections were incubated with DAB as a chromogen for 1 min. After being washed with water, the sections were observed under a microscope (BZ-9000, KEYENCE).

4.6. *In vitro* autoradiography of AD brain sections

This experiment was performed according to the method reported previously.[27] The serial sections used in immunohistochemical staining were used for this study. Deparaffinization was carried out according to the protocol described above. The sections were incubated with radiofluorinated chalcones (370 kBq/mL in 10% EtOH) for 1 h at room temperature. They were then washed in 50% EtOH for 3 min twice.

After drying, the ^{18}F-labeled sections were exposed to a BAS imaging plate (Fuji Film) for 12 h. Autoradiographic images were obtained by using a BAS5000 scanner system (Fuji Film).

4.7. Measurement of log P values

The determination of partition coefficient values were performed in 1-octanol and PBS (−) at a pH of 7.4. 1-Octanol (3.0 mL) and PBS (−) (3.0 mL) were pipetted into a 15-mL-test tube containing 0.40 MBq of test compounds. The test tube was vortexed for 2 min, and centrifuged (10 min, 2000 rpm). Aliquots (500 μL) from the 1-octanol and PBS (−) phases were transferred into two test tubes for counting. The remaining 1-octanol phase was transferred (1.0 mL) into a new test tube. 1-Octanol (2.0 mL) and PBS (−) (3.0 mL) were pipetted into the test tube. The vortexing, centrifuging, and counting were repeated. The amount of radioactivity in each tube was measured with a γ counter (Perkin Elmer, Wizard 1470). The partition coefficient was calculated using Eq. 1:

(counts/μL in 1-octanol)/(counts/μL in PBS(-)) = r (1)

Acknowledgments

This research was supported by JSPS KAKENHI Grant Numbers JP15H01555, JP17H04260, JP17H05092, and JP17H05694.

Conflicts of interest

The authors declare that there are no conflicts of interest.

Supplementary data

Supplementary data (general information for small-animal μPET and procedure for radiofluorination, *in vivo* PET imaging of a normal mouse, and *in vitro* ARG with control human brain sections) associated with this article can be found online.

References

1. Prince M, Comans-Herrera A, Knapp M, Guerchet M, Karagiannidou M. World Alzheimer Report 2016: Improving Healthcare for People Living with Dementia, Alzheimer's Disease International, London, UK. 2016.

2. 2017 Alzheimer's disease facts and figures. *Alzheimer's & Dementia: The Journal of the Alzheimer's Association.* 2017;13:325-373.

3. Selkoe DJ. Alzheimer's disease: genes, proteins, and therapy. *Physiol Rev.* 2001;81:741-766.

4. Selkoe DJ. Alzheimer's disease: a central role for amyloid. *J Neuropathol Exp Neurol.* 1994;53:438-447.

5. Villemagne VL, Dore V, Burnham SC, Masters CL, Rowe CC. Imaging tau and amyloid-β proteinopathies in Alzheimer disease and other conditions. *Nat Rev Neurol.* 2018.

6. Koole M, Lewis DM, Buckley C, Nelissen N, Vandenbulcke M, Brooks DJ, Vandenberghe R, Van Laere K. Whole-body biodistribution and radiation dosimetry of ^{18}F-GE067: a radioligand for in vivo brain amyloid imaging. *J Nucl Med.* 2009;50:818-822.

7. Rowe CC, Ackerman U, Browne W, Mulligan R, Pike KL, O'Keefe G, Tochon-Danguy H, Chan G, Berlangieri SU, Jones G, Dickinson-Rowe KL, Kung HP, Zhang W, Kung MP, Skovronsky D, Dyrks T, Holl G, Krause S, Friebe M, Lehman L, Lindemann S, Dinkelborg LM, Masters CL, Villemagne VL. Imaging of amyloid β in Alzheimer's disease with ^{18}F-BAY94-9172, a novel PET tracer: proof of mechanism. *Lancet Neurol.* 2008;7:129-135.

8. Choi SR, Golding G, Zhuang Z, Zhang W, Lim N, Hefti F, Benedum TE,

Kilbourn MR, Skovronsky D, Kung HF. Preclinical properties of ^{18}F-AV-45: a PET agent for Aβ plaques in the brain. *J Nucl Med.* 2009;50:1887-1894.

9. Villemagne VL, Ong K, Mulligan RS, Holl G, Pejoska S, Jones G, O'Keefe G, Ackerman U, Tochon-Danguy H, Chan JG, Reininger CB, Fels L, Putz B, Rohde B, Masters CL, Rowe CC. Amyloid imaging with ^{18}F-florbetaben in Alzheimer disease and other dementias. *J Nucl Med.* 2011;52:1210-1217.

10. Wong DF, Rosenberg PB, Zhou Y, Kumar A, Raymont V, Ravert HT, Dannals RF, Nandi A, Brasic JR, Ye W, Hilton J, Lyketsos C, Kung HF, Joshi AD, Skovronsky DM, Pontecorvo MJ. In vivo imaging of amyloid deposition in Alzheimer disease using the radioligand ^{18}F-AV-45 (Florbetapir F 18). *J Nucl Med.* 2010;51:913-920.

11. Ono M, Hori M, Haratake M, Tomiyama T, Mori H, Nakayama M. Structure-activity relationship of chalcones and related derivatives as ligands for detecting of β-amyloid plaques in the brain. *Bioorg Med Chem.* 2007;15:6388-6396.

12. Fuchigami T, Yamashita Y, Haratake M, Ono M, Yoshida S, Nakayama M. Synthesis and evaluation of ethyleneoxylated and allyloxylated chalcone derivatives for imaging of amyloid β plaques by SPECT. *Bioorg Med Chem.* 2014;22:2622-2628.

13. Li Z, Cui M, Dai J, Wang X, Yu P, Yang Y, Jia J, Fu H, Ono M, Jia H, Saji H, Liu B. Novel cyclopentadienyl tricarbonyl complexes of ^{99m}Tc mimicking chalcone as

potential single-photon emission computed tomography imaging probes for β-amyloid plaques in brain. *J Med Chem.* 2013;56:471-482.

14. Ono M, Watanabe R, Kawashima H, Cheng Y, Kimura H, Watanabe H, Haratake M, Saji H, Nakayama M. Fluoro-pegylated chalcones as positron emission tomography probes for in vivo imaging of β-amyloid plaques in Alzheimer's disease. *J Med Chem.* 2009;52:6394-6401.

15. Cui M, Ono M, Kimura H, Liu BL, Saji H. Synthesis and biological evaluation of indole-chalcone derivatives as β-amyloid imaging probe. *Bioorg Med Chem Lett.* 2011;21:980-982.

16. Ono M, Ikeoka R, Watanabe H, Kimura H, Fuchigami T, Haratake M, Saji H, Nakayama M. Synthesis and evaluation of novel chalcone derivatives with ^{99m}Tc/Re complexes as potential probes for detection of β-amyloid plaques. *ACS Chem Neurosci.* 2010;1:598-607.

17. Ono M, Haratake M, Mori H, Nakayama M. Novel chalcones as probes for in vivo imaging of β-amyloid plaques in Alzheimer's brains. *Bioorg Med Chem.* 2007;15:6802-6809.

18. Ermert J. ^{18}F-labelled intermediates for radiosynthesis by modular build-up reactions: newer developments. *Biomed Res Int.* 2014;2014:812973.

19. Stephenson NA, Holland JP, Kassenbrock A, Yokell DL, Livni E, Liang SH, Vasdev N. Iodonium ylide-mediated radiofluorination of ^{18}F-FPEB and validation for human use. *J Nucl Med.* 2015;56:489-492.

20. Sander K, Gendron T, Yiannaki E, Cybulska K, Kalber TL, Lythgoe MF, Arstad E. Sulfonium salts as leaving groups for aromatic labelling of drug-like small molecules with fluorine-18. *Sci Rep.* 2015;5:9941.

21. Mossine AV, Brooks AF, Makaravage KJ, Miller JM, Ichiishi N, Sanford MS, Scott PJ. Synthesis of [^{18}F]Arenes via the Copper-Mediated [^{18}F]Fluorination of Boronic Acids. *Org Lett.* 2015;17:5780-5783.

22. Preshlock S, Calderwood S, Verhoog S, Tredwell M, Huiban M, Hienzsch A, Gruber S, Wilson TC, Taylor NJ, Cailly T, Schedler M, Collier TL, Passchier J, Smits R, Mollitor J, Hoepping A, Mueller M, Genicot C, Mercier J, Gouverneur V. Enhanced copper-mediated ^{18}F-fluorination of aryl boronic esters provides eight radiotracers for PET applications. *Chem Commun (Camb).* 2016;52:8361-8364.

23. Tredwell M, Preshlock SM, Taylor NJ, Gruber S, Huiban M, Passchier J, Mercier J, Genicot C, Gouverneur V. A general copper-mediated nucleophilic ^{18}F fluorination of arenes. *Angew Chem Int Ed Engl.* 2014;53:7751-7755.

24. Shinokubo H. Transition metal catalyzed borylation of functional π -systems. *Proc Jpn Acad Ser B Phys Biol Sci.* 2014;90:1-11.

25. Ono M, Saji H. SPECT Imaging Agents for Detecting Cerebral β-Amyloid Plaques. *Int J Mol Imaging.* 2011;2011:543267.

26. Ono M, Doi Y, Watanabe H, Ihara M, Ozaki A, Saji H. Structure-activity relationships of radioiodinated diphenyl derivatives with different conjugated double bonds as ligands for α-synuclein aggregates. *RSC Advances.* 2016;6:44305-44312.

27. Matsumura K, Ono M, Kitada A, Watanabe H, Yoshimura M, Iikuni S, Kimura H, Okamoto Y, Ihara M, Saji H. Structure-Activity Relationship Study of Heterocyclic Phenylethenyl and Pyridinylethenyl Derivatives as Tau-Imaging Agents That Selectively Detect Neurofibrillary Tangles in Alzheimer's Disease Brains. *J Med Chem.* 2015;58:7241-7257.

28. Zhuang ZP, Kung MP, Wilson A, Lee CW, Plossl K, Hou C, Holtzman DM, Kung HF. Structure-activity relationship of imidazo[1,2-a]pyridines as ligands for detecting β-amyloid plaques in the brain. *J Med Chem.* 2003;46:237-243.

29. Okamura N, Harada R, Furumoto S, Arai H, Yanai K, Kudo Y. Tau PET imaging in Alzheimer's disease. *Curr Neurol Neurosci Rep.* 2014;14:500.

30. Mason NS, Mathis CA, Klunk WE. Positron emission tomography radioligands

for in vivo imaging of Aβ plaques. *J Labelled Comp Radiopharm.* 2013;56:89-95.

31. Yoshimura M, Ono M, Matsumura K, Watanabe H, Kimura H, Cui M, Nakamoto Y, Togashi K, Okamoto Y, Ihara M, Takahashi R, Saji H. Structure-Activity Relationships and in Vivo Evaluation of Quinoxaline Derivatives for PET Imaging of β-Amyloid Plaques. *ACS Med Chem Lett.* 2013;4:596-600.

32. Vallabhajosula S. Positron emission tomography radiopharmaceuticals for imaging brain beta-amyloid. *Semin Nucl Med.* 2011;41;283-299.

33. Klunk WE, Lopresti BJ, Ikonomovic MD, Lefterov IM, Koldamova RP, Abrahamson EE, Debnath ML, Holt DP, Huang G-f, Shao L, DeKosky ST, Price JC, Mathis CA. Binding of the Positron Emission Tomography Tracer Pittsburgh Compound-B Reflects the Amount of Amyloid-β in Alzheimer's Disease Brain But Not in Transgenic Mouse Brain. *The Journal of Neuroscience.* 2005;25:10598-10606.

34. Snellman A, Lopez-Picon FR, Rokka J, Salmona M, Forloni G, Scheinin M, Solin O, Rinne JO, Haaparanta-Solin M. Longitudinal amyloid imaging in mouse brain with ^{11}C-PIB: comparison of APP23, Tg2576, and APP_{swe}-$PS1_{dE9}$ mouse models of Alzheimer disease. *J Nucl Med.* 2013;54:1434-1441.

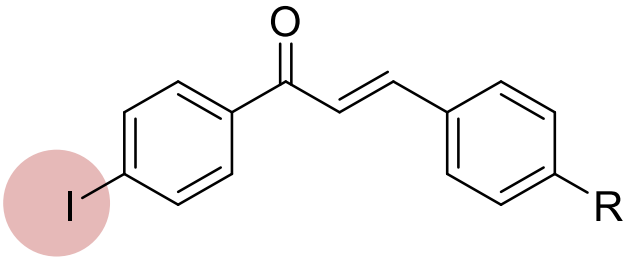

R: NMe_2, NHMe

Conversion

For β-Amyloid PET Imaging

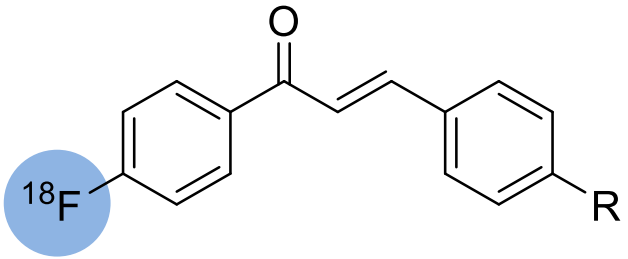

Alzheimer's Disease

Healthy Control

Human Brain Sections